Mg-dechelation of chlorophyll *a* by Stay-Green activates chlorophyll *b* degradation through expressing *Non-Yellow Coloring 1* in *Arabidopsis thaliana*

Abstract

The first step in chlorophyll *a* degradation is the extraction of the central Mg. This reaction is catalyzed by Mg-dechelatase encoded by *Stay-Green* (*SGR*) in land plants. SGR extracts Mg from chlorophyll *a* but not from chlorophyll *b*, and chlorophyll *b* must be converted to chlorophyll *a* before degradation. The first reaction of the chlorophyll *b* to chlorophyll *a* conversion is catalyzed by chlorophyll *b* reductase. Non-Yellow Coloring 1 (NYC1) and NYC1 like (NOL) are isozymes of chlorophyll *b* reductase. When *SGR* was transiently overexpressed in *Arabidopsis*, both chlorophyll *a* and *b* were degraded, suggesting that the chlorophyll *b* to chlorophyll *a* conversion is activated by *SGR* overexpression. To examine the involvement of chlorophyll *b* reductases in SGR-induced chlorophyll *b* degradation, *SGR* was transiently overexpressed in *nyc1*, *nol*, and *nyc1 nol* double mutants by dexamethasone treatment. It was found that in the wild type and *nol* mutant, chlorophyll *a* and *b* were degraded and all the chlorophyll-binding proteins decreased. Meanwhile, in *nyc1* and *nyc1 nol* mutants, chlorophyll *b* degradation was suppressed and the light-harvesting complex of photosystem II remained. The mRNA and protein levels of NYC1 increased after *SGR* overexpression in wild type plants. These results suggest that Mg-dechelation of chlorophyll *a* by SGR activates chlorophyll *b* degradation by inducing the expression of *NYC1*. This is an effective regulation of a metabolic pathway.

Introduction

Land plants and green algae have chlorophyll *a* and *b* as their photosynthetic pigments. Chlorophyll *b* is synthesized from chlorophyll *a* by oxygenation of its C-7 methyl group into a formyl group (Fig. 1). In the degradation process of chlorophyll *b*, chlorophyll *b* has to be converted to chlorophyll *a*, because chlorophyll derivatives with C-7 formyl groups are not catalyzed in the later steps of chlorophyll degradation (Hortensteiner et al., 1995). The conversion of chlorophyll *b* to chlorophyll *a* proceeds by two successive reductions. The formyl group of chlorophyll *b* is reduced by chlorophyll *b* reductase to a hydroxymethyl group to produce 7-hydroxymethyl chlorophyll *a*. There are two isozymes of chlorophyll *b* reductase, Non-Yellow Coloring 1 (NYC1) and NYC1-like (NOL) (Kusaba et al., 2007). 7-Hydroxymethyl chlorophyll *a* is then reduced to chlorophyll *a* (Meguro et al., 2011). The extraction of the central Mg by Mg-dechelatase is the first step in chlorophyll *a* degradation and pheophytin *a* is produced. Mg-dechelatase is encoded by *Stay-Green* (*SGR*) (Shimoda et al., 2016). The phytyl group of pheophytin *a* is hydrolyzed by pheophytinase to produce pheophorbide *a* (Schelbert et al., 2009), and the tetrapyrrole ring structure of pheophorbide *a* is opened by pheophorbide *a* oxygenase (Pruzinska et al., 2003). The phytyl group of chlorophyll

can be hydrolyzed by chlorophyll dephytylase during chlorophyll turnover at steady state (Lin et al., 2016).

Defects in chlorophyll degradation are a cause of delayed leaf senescence. A gene responsible for stay-green was proposed based on comparative genomics using *Lolium* / *Festuca* forage (Armstead et al., 2006) and was identified from rice and *Arabidopsis SGR* mutants (Park et al., 2007; Ren et al., 2007). *SGR* was also found to be the gene responsible for Mendel's green-cotyledon peas in the same year (Sato et al., 2007). Subsequently, many studies of *SGR* transformants were conducted and *SGR* expression under various conditions was examined (Hortensteiner, 2009; Kusaba et al., 2013). The molecular function of the gene, however, was not known. Last year, *SGR* was revealed to be an Mg-dechelatase (Matsuda et al., 2016; Shimoda et al., 2016). *SGR* is found in the genomes of green algae and land plants. In flowering plants, *SGR* homologs are classified into two subfamilies, the *SGR* subfamily and the *SGR-like* (*SGRL*) subfamily (Rong et al., 2013). *SGRL* is expressed in the developmental stage (Sakuraba et al., 2014b) and catalyzes a reaction from chlorophyll *a* and chlorophyllide *a* to pheophytin *a* and pheophorbide *a*, respectively (Shimoda et al., 2016). *SGR* is expressed in the senescent stage and catalyzes a reaction only from chlorophyll *a* to pheophytin *a*. Both subfamilies do not use chlorophyll *b* as substrate. Chlorophyll *b* tightly holds Mg (Saga and Tamiaki, 2012), and SGR is thus not able to extract Mg from chlorophyll *b*. Conversion of chlorophyll *b* to chlorophyll *a* serves to loosen the Mg and eventually the Mg is extracted by SGR.

Chlorophyll metabolic intermediates are potential photosensitizers, so the chlorophyll metabolic pathway needs to be strictly regulated. Internal regulation is one possible mechanism for strict regulation of chlorophyll metabolism. To understand the internal regulation of chlorophyll biosynthetic pathway, the expression of the genes involved in chlorophyll biosynthesis are experimentally modulated. Suppression of one gene often decreases the expression of other genes (Brzezowski et al., 2015). On the other hand, overexpression of one gene does not always increase the expression of other genes. Overexpression of Mg-protoporphyrin IX methyltransferase or NADPH-protochlorophyllide reductase affects the expression of other genes (Alawady and Grimm, 2005; Pattanayak and Tripathy, 2011). However, overexpression of glutamyl t-RNA reductase or chlorophyll synthase does not (Schmied et al., 2011; Shalygo et al., 2009). Although many examples for internal regulation are reported, our knowledge of the molecular mechanism is very limited.

When *SGR* is transiently overexpressed in *Arabidopsis*, both chlorophyll *a* and *b* are degraded (Shimoda et al., 2016). Considering that chlorophyll *b* must be converted to chlorophyll *a* before degradation, chlorophyll *b* to chlorophyll *a* conversion must be induced by *SGR* overexpression. *SGR*-overexpressing plants are therefore a good tool to explore the concerted regulation of the chlorophyll degradation pathway. In this report, chlorophyll degradation under *SGR* overexpression was investigated, and it was found that Mg-dechelation of chlorophyll *a* by SGR

induced the expression of *NYC1* and chlorophyll *b* was more rapidly degraded.

Materials and methods

Plant materials and growth conditions

Arabidopsis thaliana (Columbia ecotype) was used for the experiments. A double mutant of chlorophyll *b* reductase (hereafter *nyc1 nol*) was obtained by crossing mutants lacking *NYC1* (SALK_091664) and *NOL* (167A10) (Horie et al., 2009). The plants were grown for 4 weeks at 23°C. To suppress diurnal changes in gene expression, plants were grown under continuous light conditions (80 µmol photons m^{-2} s^{-1}).

To induce *SGR* expression chemically in *Arabidopsis*, *SGR* was expressed under the control of the pOp6 promoter and the synthetic transcription factor LhGR (Craft et al., 2005; Wielopolska et al., 2005). *SGR* cDNA with a C-terminal FLAG-tag was introduced into a binary vector, pOpON, which was constructed from the pOpOff2 vector as previously described (Shimoda et al., 2016). This construct was transferred into wild type (WT), *nyc1*, *nol*, and *nyc1 nol* plants. Plants were sprayed with dexamethasone (DEX) (10 µM) supplemented with 0.015% Silwet L-77. Mock treatment consisted of a Silwet L-77 solution. For the dark-induced leaf senescence experiments, leaf disks (0.5 cm^2) of 4-week-old plants were kept in darkness at 23°C for 9 days to degrade chlorophyll almost completely.

Pigment analysis

Pigments were extracted from leaf disks (0.5 cm^2) with 100% acetone and then separated and quantified by HPLC using a C8 column (Water Symmetry C8, Waters) with an eluent (methanol:acetonitrile:acetone [1:2:1 v:v:v]) at a flow rate of 1 mL min^{-1} at 40°C. Pigments were monitored with a diode array detector (SPD-M 10AVP; Shimadzu) with 663-nm absorbance for chlorophyll *a* and 646-nm absorbance for chlorophyll *b* (Shimoda et al., 2016). Pigment content was normalized by leaf area.

Immunoblotting analysis

Each leaf disk (0.5 cm^2) was frozen in liquid nitrogen and disrupted by shaking with tungsten beads. Proteins were extracted with 200 µL of protein extraction buffer (125 mM Tris-HCl, pH 6.8, 2% [w/v] SDS, 5% [w/v] sucrose, 2.5% [w/w] 2-mercaptoethanol). After centrifugation (22,500 *g*, 5 min), the supernatant was subjected to SDS-PAGE and then transferred onto a polyvinylidene difluoride membrane for immunoblotting analysis as described previously (Shimoda et al., 2016). All of the target proteins were detected using a primary antibody from Agrisera, except for the antibody against FLAG-tag (Sigma-Aldrich) (Shimoda et al., 2016). The primary antibodies were diluted with an immunoreaction enhancer solution (Can Get Signal, Toyobo). Anti-rabbit IgG linked

to horseradish peroxidase was used as the secondary antibody. Horseradish peroxidase activity was visualized using a Western Lightning Plus-ECL Chemiluminescence Detection Kit (PerkinElmer). Five µL of the supernatant was used to detect PsaB, PsaC, Lhca1, D1, CP43, Lhcb2, and Lhcb4. Ten µL of the supernatant was used to detect FLAG, NYC1, and NOL. For Coomassie Brilliant Blue (CBB) staining, 10 µL of the supernatant was used.

RNA isolation and semi-quantitative real-time PCR analysis

RNA was extracted from leaf tissues using an RNeasy Mini Kit (Qiagen). The cDNA was synthesized using a PrimeScriptRT Reagent Kit with gDNA eraser (Takara). Semi-quantitative real-time PCR was performed using SsoAdvanced Universal SYBR Green Supermix (BioRad) and a MyiQ2 (BioRad). The *actin 2* (*ACT2*) gene (5'-CGT ACA ACC GGT ATT GTG CT-3', 5'-CAG TAA GGT CAC GTC CAG CA-3') was used as an internal control to standardize the levels of *SGR* (5'-CAT TGT CAC ATA AGC GGT GG-3', 5'-AGT TCC CAT CTC CAT GCA C-3'), *NYC1* (5'-TTG ATG ACC AAG GAC GGG CGT TA-3', 5'-GCT TTG TAA GAT GAT GAA AGC GCA-3'), and *NOL* (5'-GCC GAG AGG CAA TGA ATA TGA T-3', 5'-CCA TAT GCA GCA AAT CTG GGT GTT-3').

Native green gel analysis and pigment measurement

Five detached leaves were homogenized in 3 mL of 50 mM Tris-HCl (pH 7.5) and 5 mM EDTA with a glass homogenizer, and centrifuged at 10,000 *g* for 5 min at 4°C. The pellet was washed twice with 5 mM EDTA. The pellet was then suspended in water (chlorophyll concentration was 0.2-1.0 mM) and mixed with the same volume of solubilizing buffer (0.6 M Tris-HCl [pH 8.8], 1% SDS, 20% [v/v] glycerol) and centrifuged at 10,000 *g* for 1 min. Ten µL of the supernatant was applied on a polyacrylamide disc gel (5 mm diameter, 8% acrylamide, 41 mM Tris-borate, pH 8.64). Electrophoresis was performed at a constant current of 0.5 mA per disc gel for 1.5 h at 4°C. The cathode buffer was 50 mM Tris-borate (pH 9.5) containing 0.1% SDS, and the anode buffer was 41 mM Tris-borate (pH 8.64) containing 0.1% SDS (Argyroudi-Akoyunoglou and Castorinis, 1980). The bands corresponding to the light-harvesting complex of the photosystem II (LHCII) trimer were excised from the gel and homogenized in the buffer (41 mM Tris-borate, pH 8.64). After centrifugation at 22,500 *g* for 5 min, the pigments contained in the supernatant were analyzed by HPLC as described above.

Transmission electron microscopy

Transmission electron microscopy observation was carried out according to the methods previously reported (Kusaba et al., 2007). HEPES buffer (60 mM HEPES-NaOH, pH 7.4, 200 mM NaCl, 4 mM $CaCl_2$) was used instead of 0.1 M cacodylate buffer. Briefly, mock- or DEX-treated leaves were

soaked in primary fixation buffer (2.5% glutaraldehyde in HEPES buffer). After rinsing three times in HEPES buffer, they were fixed with secondary fixation buffer (1% OsO_4 in HEPES buffer). The samples were dehydrated in a gradient series of ethanol and propylene oxide, and then embedded in an epon resin mixture (TAAB Epon 812, TAAB). Ultrathin sections were stained with EM stainer (Nisshin EM) and 2% (w/v) lead citrate. Photographs were taken using a transmission electron microscope (H-7650, Hitachi).

Results

Changes in chlorophyll levels after induction of SGR

There are three *SGR* homologs in *Arabidopsis* (AT1G44000, AT4G11910, AT4G22920). *SGR* encoded by AT4G22920 (*SGR1*, also known as *NYE1*) is the major *SGR* expressed in senescent leaves (Sakuraba et al., 2014b). Therefore, SGR encoded by AT4G22920 was used to explore the effect of SGR overexpression on chlorophyll metabolism. Constitutive overexpression of *SGR* causes extensive damage to plants (Park et al., 2007). To determine the primary effect of *SGR* expression on chlorophyll degradation, inducible overexpression of *SGR* was employed. DEX-inducible *SGR* was introduced into WT *Arabidopsis* plants (*SGR*/WT). DEX was applied to 4-week-old plants and the chlorophyll levels were determined every 12 h (Fig. 2A). Both the chlorophyll *a* and *b* levels decreased up to 48 h. SGR cannot catalyze chlorophyll *b*, and so NYC1 or NOL are considered to be involved in chlorophyll *b* degradation by DEX treatment. Previously, suppression of chlorophyll *b* degradation was reported in *nyc1 nol* mutant plants after *SGR* overexpression (Shimoda et al., 2016). This also supports the idea that NYC1 or NOL converts chlorophyll *b* to chlorophyll *a* after *SGR* overexpression. To examine which chlorophyll *b* reductase is involved in chlorophyll *b* degradation, *SGR* was expressed in *nyc1* mutant (*SGR*/*nyc1*), *nol* mutant (*SGR*/*nol*), and *nyc1 nol* double mutant (*SGR*/*nyc1 nol*) plants. When *SGR* was expressed in *SGR*/*nyc1* and *SGR*/*nyc1 nol*, chlorophyll *b* degradation was suppressed (Fig. 2A). These observations were confirmed by the independent transgenic lines (Supplemental Fig.S1). These observations confirm that NYC1 must convert chlorophyll *b* to chlorophyll *a* for SGR-induced chlorophyll *b* degradation.

It was found that changes in chlorophyll content as a result of DEX treatment varied depending on the plants, and this variation may have been caused by different levels of *SGR* expression as a result of the DEX treatment. This makes it difficult to understand the exact changes in chlorophyll *b* content if chlorophyll content levels are simply averaged. To compare the degradation of chlorophyll *a* with that of chlorophyll *b*, the chlorophyll *a* and chlorophyll *b* levels of WT and mutant plants were drawn as scatter plots (Fig. 2B). In *SGR*/WT, chlorophyll *a* and chlorophyll *b* were similarly degraded. *SGR*/*nol* showed a similar profile to SGR/WT. In *SGR*/*nyc1* and *SGR*/*nyc1 nol*, the decrease in chlorophyll *b* content was not proportional to that in chlorophyll *a*

content but chlorophyll *b* content remained at an almost constant level. These observations suggest that chlorophyll *b* was not degraded as efficiently as chlorophyll *a* in *SGR*/*nyc1* and *SGR*/*nyc1 nol*. Defect in chlorophyll *b* degradation was also found in *SGR*/*nyc1* and *SGR*/*nyc1 nol* mutant plants after dark treatment (Fig. 2C) (Horie et al., 2009). NYC1 is the major chlorophyll *b* reductase, when chlorophyll *b* degradation is activated.

Chlorophyll-binding protein levels after induction of SGR

Changes in photosystem protein levels after DEX treatment were examined by immunoblotting analysis (Fig. 3A). PsaB and PsaC are the components of the photosystem (PS) I core complex. Lhca1 is the peripheral light-harvesting complex of PSI. All of these proteins decreased in *SGR*/WT and *SGR*/*nyc1 nol* plants after DEX treatment. D1 and CP43 are the components of the PSII core complex. Lhcb2 and Lhcb4 are the major and minor peripheral light-harvesting complex of PSII, respectively. Both D1 and CP43 decreased in *SGR*/WT and *SGR*/*nyc1 nol* plants after DEX treatment. Degradation profiles of Lhcb2 and Lhcb4 were different between *SGR*/WT and *SGR*/*nyc1 nol*. In *SGR*/WT, Lhcb2 and Lhcb4 decreased after DEX treatment, whereas their decrease was suppressed in *SGR*/*nyc1 nol* plants. CBB staining also showed suppression of LHCII degradation in *SGR*/*nyc1 nol* plants (Fig. 3B). Mock treatment did not have any effect on the protein profiles. These observations suggest that conversion of chlorophyll *b* to chlorophyll *a* is indispensable for SGR-induced LHCII degradation.

Chlorophyll composition in the LHCII trimer

Chlorophyll-binding protein complexes were separated by native green gel electrophoresis to determine the chlorophyll *a*/*b* ratio of LHCII. In WT and mock-treated *SGR*/*nyc1 nol*, bands were observed for CP1 (PsaA/B complex), CP1* (CP1-LHCI complex), trimeric and monomeric LHCII, and CP43/CP47 (Fig. 4A). After DEX treatment, LHCII was selectively stabilized in *SGR*/*nyc1 nol*. This is consistent with the immunoblotting analysis and CBB staining. Green bands corresponding to the LHCII trimer were excised, and chlorophylls were extracted and analyzed by HPLC. The chlorophyll *a*/*b* ratio of the LHCII trimer from DEX-treated leaves of *SGR*/*nyc1 nol* was 0.54 (Fig. 4B). This was much lower than that of WT (1.35) and mock-treated *SGR*/*nyc1 nol* plants (1.26). About half of the chlorophyll *a* in LHCII was degraded by SGR in *SGR*/*nyc1 nol*. These observations suggest that SGR can catalyze a fraction of the chlorophyll *a* in LHCII, which is different from the core antenna complex. It should be noted that when LHCII loses part of its chlorophyll *a*, it can still be stabilized in the thylakoid membrane.

Ultrastructure of chloroplasts after induction of SGR

The ultrastructure of the chloroplasts was examined with an electron microscope to determine the

effect of chlorophyll degradation on chloroplast membrane structure. *SGR*/WT and *SGR*/*nyc1 nol* plants without DEX treatment did not show any obvious differences in chloroplast structure (Fig. 5). After DEX treatment, most of the thylakoid membrane including the grana stack and stromal thylakoid disappeared in *SGR*/WT, whereas thick grana stacks were found in *SGR*/ *nyc1 nol*. The stroma thylakoid membrane was degraded in the *SGR*/*nyc1 nol* chloroplasts. LHCII still remained in *SGR*/*nyc1 nol* after DEX treatment (Fig. 4A). It is hypothesized that LHCII stabilizes grana stack structure. Stacked grana structures have been observed in a chlorophyll *b* reductase mutant of rice after dark treatment (Kusaba et al., 2007). NYC1 is proposed to contribute to an important role in the degradation of photosystem and chloroplast membranes due to chlorophyll *b* reduction to chlorophyll *a*.

Expression of *SGR* and *NYC1*

As described above, NYC1 is indispensable for SGR-induced chlorophyll *b* degradation. The NYC1 protein levels are very low or undetectable during the developmental phase because chlorophyll *b* does not need to be degraded, but they increase during senescence (Jia et al., 2015). This indicates that NYC1 levels are too low for chlorophyll *b* degradation in green leaves and that *NYC1* must be upregulated for SGR-induced chlorophyll *b* degradation. To determine whether *NYC1* is induced after *SGR* overexpression, the protein and mRNA levels of *NYC1* and related genes were examined. SGR was expressed with a FLAG tag and was detected using anti-FLAG antibody. SGR accumulated after 12 h of DEX treatment in both *SGR*/WT and *SGR*/*nyc1 nol* plants (Fig. 6). FLAG band intensities of *SGR*/*nyc1 nol* were stronger than those of *SGR*/WT. Responses to DEX are not completely same among plants. The difference of SGR levels may not depend on the genotype of plants. Before DEX treatment, NYC1 protein was barely detectable. After DEX treatment, the NYC1 protein levels increased up to 36 h. The NYC1 protein expression by DEX treatment was also observed in another independent transgenic line (Supplemental Fig. S2). These observations demonstrated that SGR accumulation induced NYC1 accumulation. The NOL protein levels were not significantly changed. In rice, NOL protein is stabilized by NYC1 protein, whereas, NOL protein and NYC1 protein stabilities are not related in *Arabidopsis* (Horie et al., 2009; Kusaba et al., 2007). Therefore, the NOL protein levels were not affected by NYC1protein accumulation after DEX treatment.

Next, mRNA levels were examined by semi-quantitative real-time PCR. *ACT2* was used to normalize the mRNA levels. mRNA was extracted every 6 h after mock or DEX treatment. SGR mRNA induction was observed after 6 h of DEX treatment and it increased gradually up to 42 h (Fig. 7). The NYC1 mRNA level increased after 12 h. After 42 h, NYC1 mRNA increased about 3-fold. Compared to the expression level of NYC1 mRNA, the amount of NYC1 protein was markedly increased, consistent with the previous report (Jia et al., 2015). Significant upregulation of NYC1

protein would be partly due to the regulation of protein stability. The NOL mRNA level was slightly decreased by DEX treatment.

Discussion

Induction of chlorophyll *b* degradation by chlorophyll *a* degradation

Chlorophyll *b* is reduced to 7-hydroxymethyl chlorophyll *a* by chlorophyll *b* reductase. This reaction is involved both in chlorophyll *b* degradation during senescence and in regulation of chlorophyll levels for photoacclimation (Kusaba et al., 2007; Sato et al., 2015). In this study, NYC1, an isozyme of chlorophyll *b* reductase, was found to be induced concomitant with chlorophyll *a* degradation by *SGR* expression. This is the effective regulation mechanism for coordinated degradation of chlorophyll *a* and *b*. In the chlorophyll biosynthetic pathway, transcriptional and post-transcriptional controls have been reported (Brzezowski et al., 2015; Tanaka et al., 2011). Post-transcriptional feedback control is especially important for chlorophyll metabolism because fine regulation is indispensable for keeping the level of chlorophyll precursors low. On the other hand, positive feedback control is not well understood. Overexpression of one gene does not always induce other genes in the chlorophyll biosynthetic pathway (Schmied et al., 2011; Shalygo et al., 2009). In the chlorophyll degradation pathway, NYC1 was found to accumulate after *SGR* expression (Fig. 6). This observation indicates the presence of positive feedback regulation of *NYC1* by *SGR* expression. This positive feedback regulation is justifiable because both chlorophyll *a* and chlorophyll *b* must be degraded during senescence, but SGR directly degrades only chlorophyll *a*. SGR can contribute to chlorophyll *b* degradation only by cooperation with NYC1.

When turf grass *SGR* is overexpressed constitutively in *Arabidopsis*, chlorophyll degradation occurs (Teng et al., 2016). Transcriptome analysis of this system shows that genes related to plant hormones such as salicylate, abscisic acid, jasmonate, and ethylene are up-regulated. *NYC1* is also up-regulated. These observations suggest that *SGR* induction accelerates senescence. However, it is not clear whether chlorophyll *a* degradation is the primary factor in differential gene expression, because plants constitutively overexpressing *SGR* are under stress, and are not able to develop their photosystems, and die (Park et al., 2007). In this study, transient expression by DEX treatment was applied and most chlorophyll was degraded within 48 h (Fig. 2A). This allowed us to examine the primary response of the plants to chlorophyll *a* degradation. *NYC1* gene expression and protein accumulation were observed after 12 h and 24 h of DEX treatment, respectively (Figs. 6, 7). SGR catalyzes the first step of chlorophyll degradation, and degradation of chlorophyll *a* may therefore be closely related to *NYC1* induction.

SGR may regulate *NYC1* expression via transcriptional factors because SGR is localized in the chloroplast and cannot directly regulate gene expression. Several transcription factors are reported to bind to the *NYC1* promoter. EIN3 is a key transcription factor in the ethylene signaling

pathway, and ORE1 is related to EIN3 function. Both transcription factors bind to the *NYC1* promoter and express *NYC1* (Qiu et al., 2015). ABF4 is an abscisic acid-responsive element-binding factor. ABF4 also binds to the *NYC1* promoter (Nakajima et al., 2012). Some other positive and negative transcription factors are known to regulate the *NYC1* gene directly (Chen et al., 2017; Liang et al., 2014; Oda-Yamamizo et al., 2016; Sakuraba et al., 2014a; Zhu et al., 2015). Regulation of these factors by *SGR* overexpression remains to be investigated.

Degradation of photosystems by SGR overexpression

Apoproteins of chlorophyll-binding protein can stably accumulate only when they bind chlorophyll. This is the reason chlorophyll-binding protein complexes disappeared after chlorophyll degradation by SGR (Fig. 3A). The core complex of the photosystem has chlorophyll *a*, whereas the peripheral light-harvesting complex has chlorophyll *a* and *b* (Nelson and Yocum, 2006). When *SGR* was overexpressed in *SGR*/*nyc1 nol*, LHCII was not degraded (Fig. 3A). This suggests that chlorophyll *b* needs to be degraded by NYC1 for LHCII degradation. Dark incubation of the *nyc1* mutant also supports this conclusion. When *nyc1* mutant plants are incubated in the dark, chlorophyll *b* and LHCII are not degraded (Horie et al., 2009). These observations lead to the conclusion that chlorophyll *b* degradation is indispensable for LHCII degradation and that NYC1, not NOL, participates in this reaction. Stacked thylakoid membranes were observed after *SGR* overexpression in *SGR*/*nyc1 nol* (Fig. 5). Immunoblotting analysis (Fig. 3A) and native green gel electrophoresis (Fig. 4A) showed the presence of LHCII after *SGR* overexpression in *SGR*/*nyc1 nol*. The remaining LHCII would be involved in this stacked grana structure. It should be noted that the level of chlorophyll *a* in LHCII decreased (Fig. 4B). This indicates that SGR can access LHCII and catalyze chlorophyll in LHCII, but it cannot degrade all the chlorophyll *a* molecules in LHCII. Chlorophyll *b* in LHCII may protect chlorophyll *a* molecules against SGR. Plants overexpressing truncated CAO are reported to exhibit the stay-green phenotype (Sakuraba et al., 2012). In these transgenic plants, a large amount of chlorophyll *b* is incorporated not only into LHC but also into the core antenna complexes. The presence of chlorophyll *b* may interfere with the function of SGR resulting in the stay-green phenotype.

In contrast to LHCII, LHCI was degraded in *SGR*/*nyc1 nol* (Fig. 3A), even though it binds chlorophyll *b* as LHCII. LHCI degradation is also observed under high light or dark treatment in *nyc1 nol*, while LHCII degradation is suppressed (Horie et al., 2009; Sato et al., 2015). These results suggest that LHCI is degraded by only chlorophyll *a* degradation (Schmid et al., 2001). LHCII (Lhcb4) carrying a mutation at a single chlorophyll-binding residue loses a single chlorophyll (Bassi et al., 1999). On the other hand, in LHCI, each mutation tends to lose more than one chlorophyll and decrease protein stability (Morosinotto et al., 2002). In *SGR*/*nyc1 nol* plants, chlorophyll *a* in LHCI is degraded by SGR resulting in the destabilization of LHCI in spite of the presence of chlorophyll *b*

(Fig. 3A). It is also reported that PSI core complex affects LHCI stability. Plants with reduced amounts of PSI core complex have less LHCI (Haldrup et al., 2003). Degradation of PSI core complex by SGR might also promote LHCI degradation without chlorophyll *b* degradation.

PsaC is a component of PSI and does not bind chlorophyll (Qin et al., 2015). After DEX treatment, PsaC decreased in both *SGR*/WT and *SGR*/*nyc1 nol* plants. PsaC would be unstable without interacting with the PSI core complex. This suggests that SGR degrades chlorophyll, resulting in the degradation of all components of the photosystem. Recombinant SGR catalyzes the chlorophyll *a* of isolated PSI and LHCII (Shimoda et al., 2016). The substrate used by SGR *in vivo* should be the chlorophyll *a* of the chlorophyll-protein complex because the degradation of chlorophyll *a* in photosystems can begin by SGR induction. These results suggest the degradation process of photosystems is as follows. The first step is the degradation of chlorophyll *a* in the core antenna complex. Then, chlorophyll-depleted apoproteins are degraded by proteases. Next, other colorless protein components such as PsaC are degraded, and finally all the photosystem components disappear. In these processes, SGR may catalyze most important regulatory step.

Conclusions

SGR is an Mg-dechelatase that catalyzes only chlorophyll *a*. When *SGR* was transiently overexpressed, both chlorophyll *a* and chlorophyll *b* were degraded, suggesting that conversion of chlorophyll *b* to chlorophyll *a* was activated. NYC1, an isozyme responsible for the first step of chlorophyll *b* to chlorophyll *a* conversion, was upregulated, with a concomitant decrease in chlorophyll *a*, by *SGR* overexpression. An *NYC1*-deficient mutant did not degrade chlorophyll *b* and LHCII under *SGR* overexpression. These observations demonstrate a strong association between chlorophyll *a* degradation and chlorophyll *b* degradation through NYC1 induction. This is a new observation of chloroplast-to-nucleus communication. Regulation of metabolic pathways is crucial for plant development. Identification of the molecules included in this communication will promote understanding of the regulation of gene expression.

Figure legends

Fig. 1 Chlorophyll metabolic pathway

SGR extracts Mg from chlorophyll *a*. NYC1 and NOL are chlorophyll *b* reductase and convert chlorophyll *b* to chlorophyll *a*.

Fig. 2 Chlorophyll content after DEX treatment

(A) Chlorophyll was extracted from leaf disks every 12 h after mock or DEX treatment. Chlorophyll content was normalized by leaf area. The error bars represent the S. D. (n = 3). (B) The chlorophyll *b* level against the chlorophyll *a* level after DEX treatment from 0 h to 48 h. Mock-treated samples are

not included. (C) Chlorophyll was extracted from leaf disks with or without dark treatment for 9 d. Chlorophyll content was normalized by leaf area. The error bars represent the S. D. (n = 3).

Fig. 3 Analysis of chlorophyll-binding protein after DEX treatment
Proteins were extracted from leaf disks of *SGR*/WT and *SGR*/*nyc1 nol* leaves every 12 h up to 48 h after DEX treatment. Leaves mock-treated for 48 h were also analyzed. The results were normalized by leaf area. (A) Each protein was detected using a specific primary antibody. (B) Proteins were stained by CBB. Rubisco large subunit (RbcL) and LHCII are indicated.

Fig. 4 Chlorophyll composition of LHCII
(A) Proteins were extracted from leaves of WT and *SGR*/*nyc1 nol* plants after mock or DEX treatment for 48 h. Chlorophyll-binding protein complexes were separated by native green gel electrophoresis. CP1 is a PsaA/B complex. CP1* is a supercomplex of CP1 and LHCI. (B) The bands corresponding to LHCII were excised from the native green gel. Chlorophyll was extracted and the chlorophyll *a*/*b* ratio was determined by HPLC analysis. N.D.; not detected.

Fig. 5 Transmission electron microscopy of chloroplast structure
SGR/WT mock treatment, *SGR*/WT DEX treatment, *SGR*/*nyc1 nol* mock treatment, *SGR*/*nyc1 nol* DEX treatment for 48 h were shown. Images on the right are enlargements of the images on the left. Scale bar = 1 μm.

Fig. 6 Protein accumulation after DEX treatment
Proteins were extracted from leaf disks of *SGR*/WT and *SGR*/*nyc1 nol* leaves every 12 h up to 48 h after mock or DEX treatment. Results were normalized by leaf area. FLAG-tagged SGR was detected using a primary antibody against FLAG tag.

Fig. 7 mRNA expression after DEX treatment
Total RNA was extracted from the mock- or DEX-treated leaves every 6 h up to 48 h. The mRNA levels were examined using specific primer sets. The mRNA level in each sample was normalized by *ACT2*. The mRNA level at 0 h was arbitrarily set to 1. The error bars represent the S. D. (n = 3). * $p<0.05$, ** $p<0.01$ (*t*-test).

Acknowledgements
We thank Junko Kishimoto for technical assistance in electron microscopy. We thank CSIRO, Max-Planck-Gesellschaft zur Forderung der Wissenschaften c.V. (MPG), and Dr. Ian Moore of the University of Oxford for providing the pOpOff vector. This work was supported by a Grant-in-Aid

for Scientific Research15H04381 (to A. T.), 17K07430 (to H. I.).

Alawady, A.E., Grimm, B., 2005. Tobacco Mg protoporphyrin IX methyltransferase is involved in inverse activation of Mg porphyrin and protoheme synthesis. Plant J. 41(2), 282-290.

Argyroudi-Akoyunoglou, J.H., Castorinis, A., 1980. Specificity of the chlorophyll-to-protein binding in the chlorophyll-protein complexes of the thylakoid. Arch. Biochem. Biophys. 200(2), 326-335.

Armstead, I., Donnison, I., Aubry, S., Harper, J., Hörtensteiner, S., James, C., Mani, J., Moffet, M., Ougham, H., Roberts, L., Thomas, A., Weeden, N., Thomas, H., King, I., 2006. From crop to model to crop: identifying the genetic basis of the staygreen mutation in the Lolium/Festuca forage and amenity grasses. New Phytol. 172(4), 592-597.

Bassi, R., Croce, R., Cugini, D., Sandonà, D., 1999. Mutational analysis of a higher plant antenna protein provides identification of chromophores bound into multiple sites. Proc. Natl. Acad. Sci. U. S. A. 96(18), 10056-10061.

Brzezowski, P., Richter, A.S., Grimm, B., 2015. Regulation and function of tetrapyrrole biosynthesis in plants and algae. Biochim. Biophys. Acta 1847(9), 968-985.

Chen, J., Zhu, X., Ren, J., Qiu, K., Li, Z., Xie, Z., Gao, J., Zhou, X., Kuai, B., 2017. Suppressor of Overexpression of CO 1 Negatively Regulates Dark-Induced Leaf Degreening and Senescence by Directly Repressing Pheophytinase and Other Senescence-Associated Genes in Arabidopsis. Plant Physiol. 173(3), 1881-1891.

Craft, J., Samalova, M., Baroux, C., Townley, H., Martinez, A., Jepson, I., Tsiantis, M., Moore, I., 2005. New pOp/LhG4 vectors for stringent glucocorticoid-dependent transgene expression in Arabidopsis. Plant J. 41(6), 899-918.

Haldrup, A., Lunde, C., Scheller, H.V., 2003. Arabidopsis thaliana Plants Lacking the PSI-D Subunit of Photosystem I Suffer Severe Photoinhibition, Have Unstable Photosystem I Complexes, and Altered Redox Homeostasis in the Chloroplast Stroma. J. Biol. Chem. 278(35), 33276-33283.

Horie, Y., Ito, H., Kusaba, M., Tanaka, R., Tanaka, A., 2009. Participation of chlorophyll b reductase in the initial step of the degradation of light-harvesting chlorophyll a/b-protein complexes in Arabidopsis. J. Biol. Chem. 284(26), 17449-17456.

Hortensteiner, S., 2009. Stay-green regulates chlorophyll and chlorophyll-binding protein degradation during senescence. Trends Plant Sci. 14(3), 155-162.

Hortensteiner, S., Vicentini, F., Matile, P., 1995. Chlorophyll breakdown in senescent cotyledons of rape, Brassica napus L.: Enzymatic cleavage of phaeophorbide a in vitro. New Phytol. 129(2), 237-246.

Jia, T., Ito, H., Hu, X., Tanaka, A., 2015. Accumulation of the NON-YELLOW COLORING 1 protein of the chlorophyll cycle requires chlorophyll b in Arabidopsis thaliana. Plant J. 81(4), 586-596.

Kusaba, M., Ito, H., Morita, R., Iida, S., Sato, Y., Fujimoto, M., Kawasaki, S., Tanaka, R., Hirochika, H.,

Nishimura, M., Tanaka, A., 2007. Rice NON-YELLOW COLORING1 is involved in light-harvesting complex II and grana degradation during leaf senescence. Plant Cell 19(4), 1362-1375.
Kusaba, M., Tanaka, A., Tanaka, R., 2013. Stay-green plants: what do they tell us about the molecular mechanism of leaf senescence. Photosynth. Res. 117(1-3), 221-234.
Liang, C., Wang, Y., Zhu, Y., Tang, J., Hu, B., Liu, L., Ou, S., Wu, H., Sun, X., Chu, J., Chu, C., 2014. OsNAP connects abscisic acid and leaf senescence by fine-tuning abscisic acid biosynthesis and directly targeting senescence-associated genes in rice. Proc. Natl. Acad. Sci. U. S. A. 111(27), 10013-10018.
Lin, Y.-P., Wu, M.-C., Charng, Y.-y., 2016. Identification of a Chlorophyll Dephytylase Involved in Chlorophyll Turnover in Arabidopsis. Plant Cell 28(12), 2974-2990.
Matsuda, K., Shimoda, Y., Tanaka, A., Ito, H., 2016. Chlorophyll a is a favorable substrate for Chlamydomonas Mg-dechelatase encoded by STAY-GREEN. Plant Physiol. Biochem. 109, 365-373.
Meguro, M., Ito, H., Takabayashi, A., Tanaka, R., Tanaka, A., 2011. Identification of the 7-hydroxymethyl chlorophyll a reductase of the chlorophyll cycle in Arabidopsis. Plant Cell 23(9), 3442-3453.
Morosinotto, T., Castelletti, S., Breton, J., Bassi, R., Croce, R., 2002. Mutation Analysis of Lhca1 Antenna Complex: LOW ENERGY ABSORPTION FORMS ORIGINATE FROM PIGMENT-PIGMENT INTERACTIONS. J. Biol. Chem. 277(39), 36253-36261.
Nakajima, S., Ito, H., Tanaka, R., Tanaka, A., 2012. Chlorophyll b reductase plays an essential role in maturation and storability of Arabidopsis seeds. Plant Physiol. 160(1), 261-273.
Nelson, N., Yocum, C.F., 2006. Structure and function of photosystems I and II. Annu. Rev. Plant Biol. 57(1), 521-565.
Oda-Yamamizo, C., Mitsuda, N., Sakamoto, S., Ogawa, D., Ohme-Takagi, M., Ohmiya, A., 2016. The NAC transcription factor ANAC046 is a positive regulator of chlorophyll degradation and senescence in Arabidopsis leaves. Scientific Reports 6, 23609.
Park, S.Y., Yu, J.W., Park, J.S., Li, J., Yoo, S.C., Lee, N.Y., Lee, S.K., Jeong, S.W., Seo, H.S., Koh, H.J., Jeon, J.S., Park, Y.I., Paek, N.C., 2007. The senescence-induced staygreen protein regulates chlorophyll degradation. Plant Cell 19(5), 1649-1664.
Pattanayak, G.K., Tripathy, B.C., 2011. Overexpression of Protochlorophyllide Oxidoreductase C Regulates Oxidative Stress in Arabidopsis. PLoS One 6(10), e26532.
Pruzinska, A., Tanner, G., Anders, I., Roca, M., Hortensteiner, S., 2003. Chlorophyll breakdown: pheophorbide a oxygenase is a Rieske-type iron-sulfur protein, encoded by the accelerated cell death 1 gene. Proc. Natl. Acad. Sci. U. S. A. 100(25), 15259-15264.
Qin, X., Suga, M., Kuang, T., Shen, J.-R., 2015. Structural basis for energy transfer pathways in the plant PSI-LHCI supercomplex. Science 348(6238), 989-995.
Qiu, K., Li, Z., Yang, Z., Chen, J., Wu, S., Zhu, X., Gao, S., Gao, J., Ren, G., Kuai, B., Zhou, X., 2015. EIN3 and ORE1 Accelerate Degreening during Ethylene-Mediated Leaf Senescence by Directly Activating Chlorophyll Catabolic Genes in Arabidopsis. PLoS Genet 11(7), e1005399.

Ren, G., An, K., Liao, Y., Zhou, X., Cao, Y., Zhao, H., Ge, X., Kuai, B., 2007. Identification of a Novel Chloroplast Protein AtNYE1 Regulating Chlorophyll Degradation during Leaf Senescence in Arabidopsis. Plant Physiol. 144(3), 1429-1441.

Rong, H., Tang, Y., Zhang, H., Wu, P., Chen, Y., Li, M., Wu, G., Jiang, H., 2013. The Stay-Green Rice like (SGRL) gene regulates chlorophyll degradation in rice. J. Plant Physiol. 170(15), 1367-1373.

Saga, Y., Tamiaki, H., 2012. Demetalation of Chlorophyll Pigments. Chemistry & Biodiversity 9(9), 1659-1683.

Sakuraba, Y., Balazadeh, S., Tanaka, R., Mueller-Roeber, B., Tanaka, A., 2012. Overproduction of chl b retards senescence through transcriptional reprogramming in Arabidopsis. Plant Cell Physiol. 53(3), 505-517.

Sakuraba, Y., Jeong, J., Kang, M.-Y., Kim, J., Paek, N.-C., Choi, G., 2014a. Phytochrome-interacting transcription factors PIF4 and PIF5 induce leaf senescence in Arabidopsis. Nature Communications 5, 4636.

Sakuraba, Y., Park, S.-Y., Kim, Y.-S., Wang, S.-H., Yoo, S.-C., Hörtensteiner, S., Paek, N.-C., 2014b. Arabidopsis STAY-GREEN2 Is a Negative Regulator of Chlorophyll Degradation during Leaf Senescence. Mol. Plant 7(8), 1288-1302.

Sato, R., Ito, H., Tanaka, A., 2015. Chlorophyll b degradation by chlorophyll b reductase under high-light conditions. Photosynth. Res. 126(2-3), 249-259.

Sato, Y., Morita, R., Nishimura, M., Yamaguchi, H., Kusaba, M., 2007. Mendel's green cotyledon gene encodes a positive regulator of the chlorophyll-degrading pathway. Proc. Natl. Acad. Sci. U. S. A. 104(35), 14169-14174.

Schelbert, S., Aubry, S., Burla, B., Agne, B., Kessler, F., Krupinska, K., Hortensteiner, S., 2009. Pheophytin pheophorbide hydrolase (pheophytinase) is involved in chlorophyll breakdown during leaf senescence in Arabidopsis. Plant Cell 21(3), 767-785.

Schmid, V.H.R., Thomé, P., Rühle, W., Paulsen, H., Kühlbrandt, W., Rogl, H., 2001. Chlorophyll b is involved in long-wavelength spectral properties of light-harvesting complexes LHC I and LHC II. FEBS Lett. 499(1-2), 27-31.

Schmied, J., Hedtke, B., Grimm, B., 2011. Overexpression of HEMA1 encoding glutamyl-tRNA reductase. J. Plant Physiol. 168(12), 1372-1379.

Shalygo, N., Czarnecki, O., Peter, E., Grimm, B., 2009. Expression of chlorophyll synthase is also involved in feedback-control of chlorophyll biosynthesis. Plant Mol. Biol. 71(4), 425-436.

Shimoda, Y., Ito, H., Tanaka, A., 2016. Arabidopsis STAY-GREEN, Mendel's Green Cotyledon Gene, Encodes Magnesium-Dechelatase. Plant Cell 28, 2147-2160.

Tanaka, R., Kobayashi, K., Masuda, T., 2011. Tetrapyrrole Metabolism in Arabidopsis thaliana. Arabidopsis Book 9, e0145.

Teng, K., Chang, Z., Li, X., Sun, X., Liang, X., Xu, L., Chao, Y., Han, L., 2016. Functional and

RNA-Sequencing Analysis Revealed Expression of a Novel Stay-Green Gene from Zoysia japonica (ZjSGR) Caused Chlorophyll Degradation and Accelerated Senescence in Arabidopsis. Front. Plant Sci. 7(1894).

Wielopolska, A., Townley, H., Moore, I., Waterhouse, P., Helliwell, C., 2005. A high-throughput inducible RNAi vector for plants. Plant Biotechnol. J. 3(6), 583-590.

Zhu, X., Chen, J., Xie, Z., Gao, J., Ren, G., Gao, S., Zhou, X., Kuai, B., 2015. Jasmonic acid promotes degreening via MYC2/3/4- and ANAC019/055/072-mediated regulation of major chlorophyll catabolic genes. Plant J. 84(3), 597-610.

Fig. 1

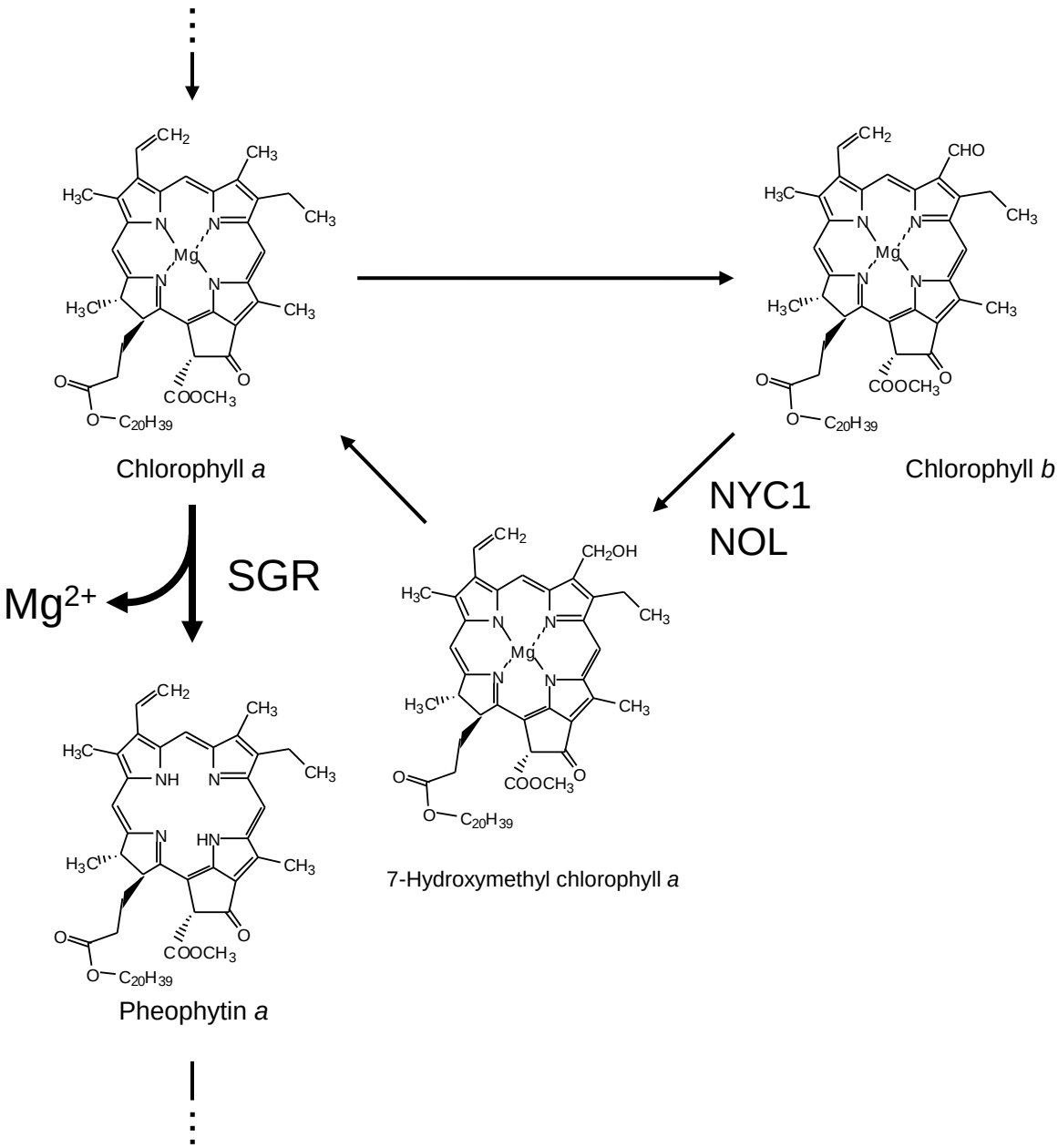
Chlorophyll a
Chlorophyll b
NYC1
NOL
Mg2+
SGR
7-Hydroxymethyl chlorophyll a
Pheophytin a

Fig. 2

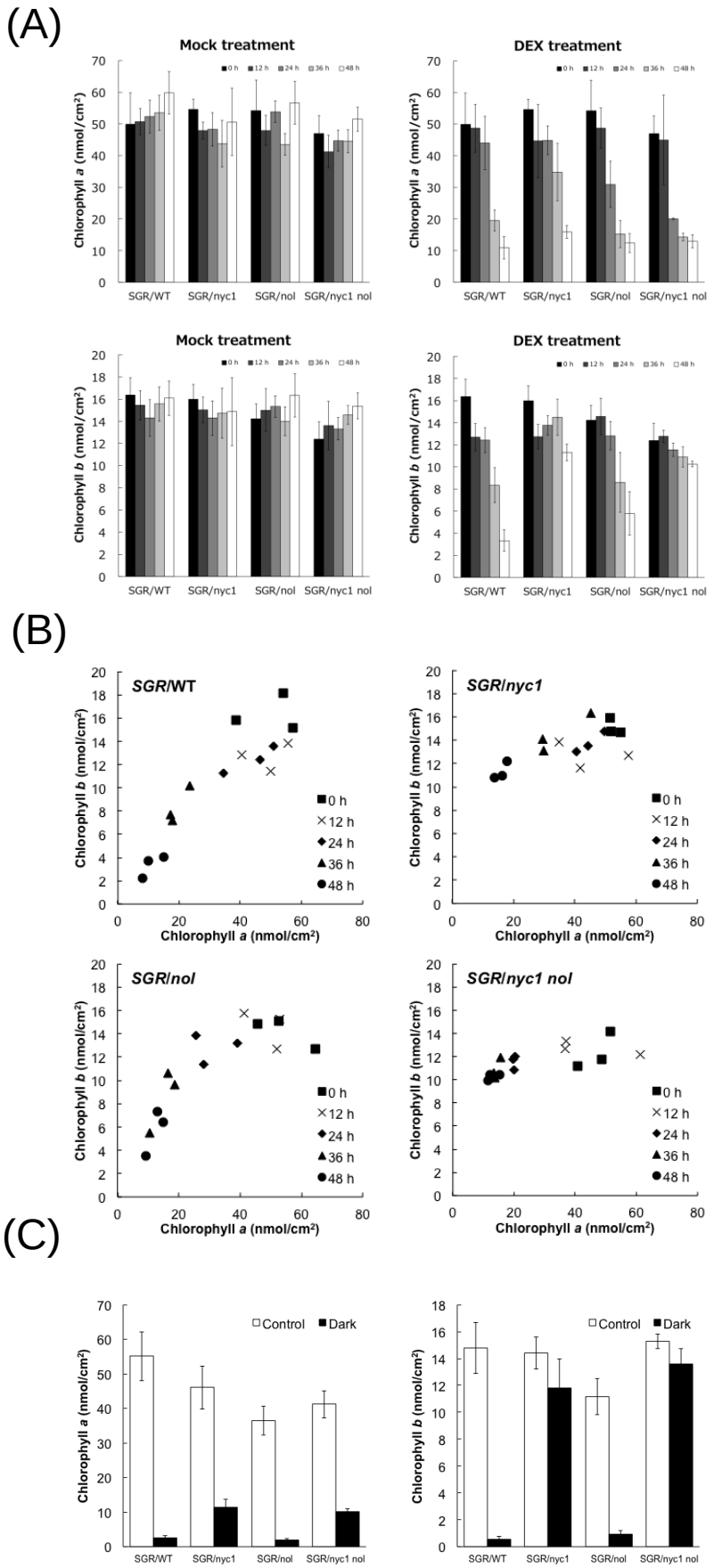
(A)
Mock treatment
DEX treatment
Chlorophyll a (nmol/cm²)
Chlorophyll b (nmol/cm²)
0 h
12 h
24 h
36 h
48 h
SGR/WT
SGR/nyc1
SGR/nol
SGR/nyc1 nol
(B)
SGR/WT
SGR/nyc1
SGR/nol
SGR/nyc1 nol
Chlorophyll a (nmol/cm²)
Chlorophyll b (nmol/cm²)
(C)
Control
Dark
Chlorophyll a (nmol/cm²)
Chlorophyll b (nmol/cm²)

Fig. 3

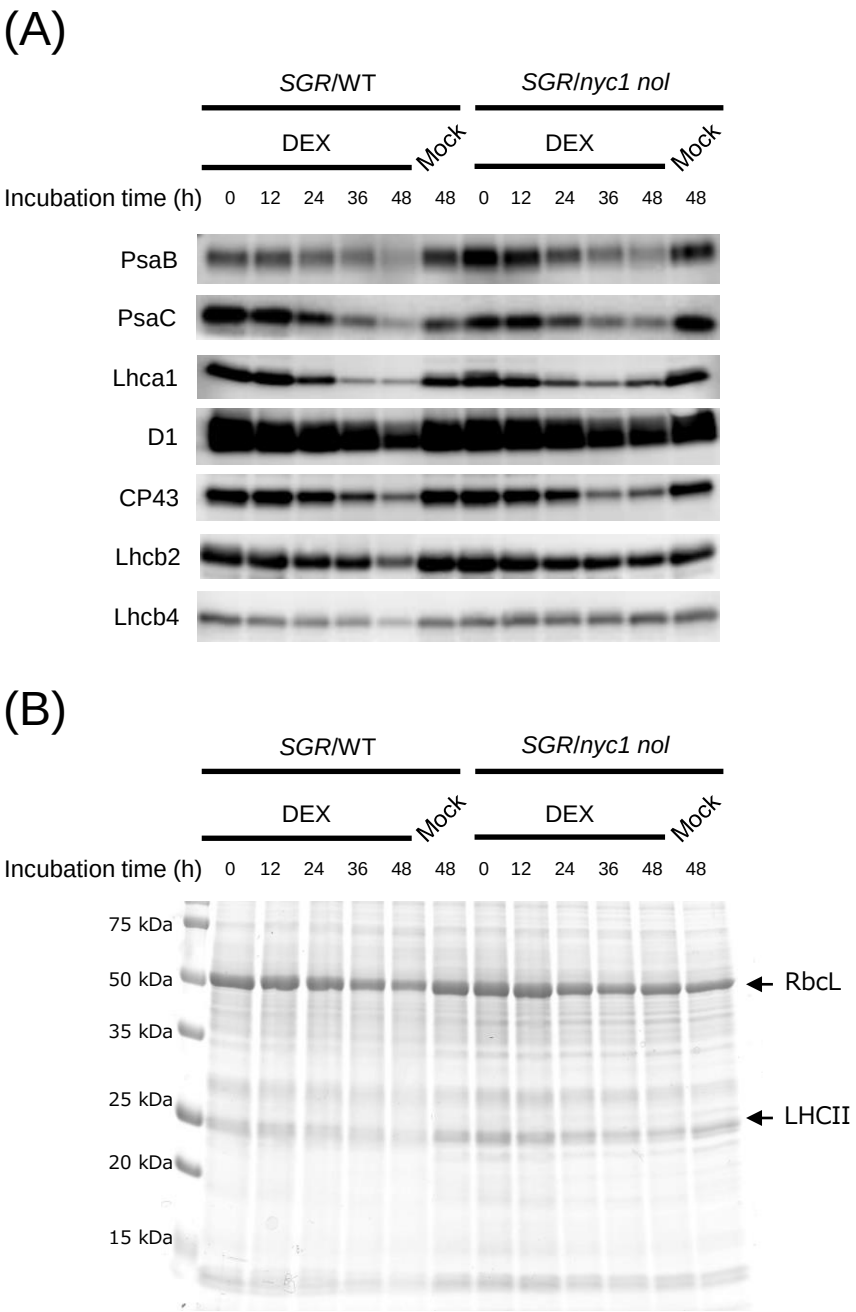
(A)
SGR/WT
SGR/nyc1 nol
DEX
Mock
DEX
Mock
Incubation time (h)
0 12 24 36 48 48 0 12 24 36 48 48
PsaB
PsaC
Lhca1
D1
CP43
Lhcb2
Lhcb4
(B)
SGR/WT
SGR/nyc1 nol
DEX
Mock
DEX
Mock
Incubation time (h)
0 12 24 36 48 48 0 12 24 36 48 48
75 kDa
50 kDa
35 kDa
25 kDa
20 kDa
15 kDa
RbcL
LHCII

Fig. 4

(A)

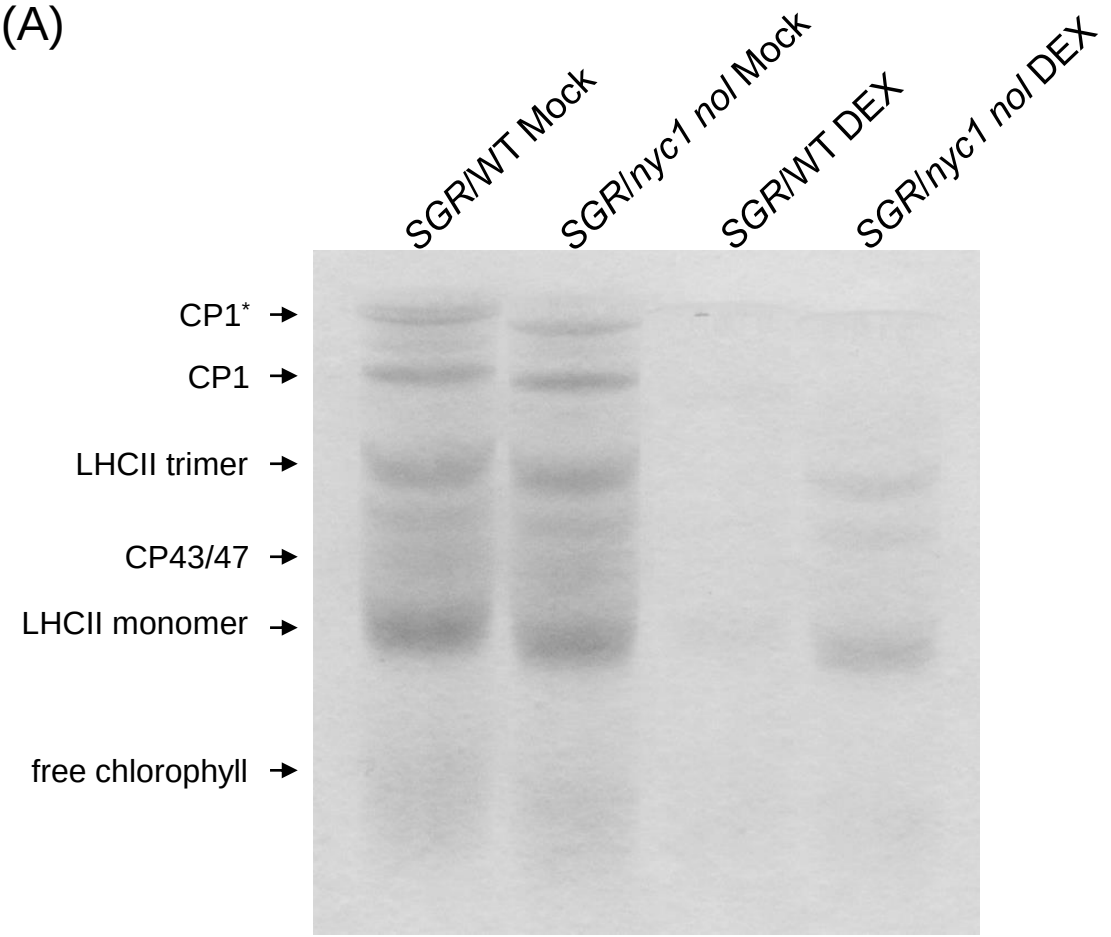
SGR/WT Mock
SGR/nyc1 nol Mock
SGR/WT DEX
SGR/nyc1 nol DEX
CP1*
CP1
LHCII trimer
CP43/47
LHCII monomer
free chlorophyll

(B)

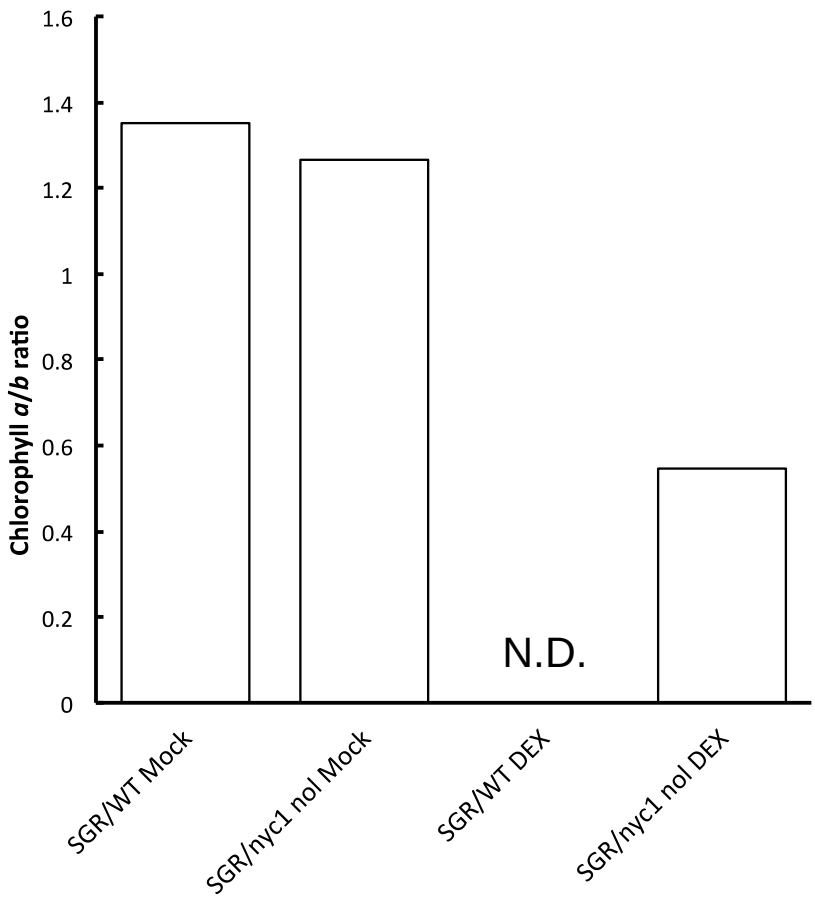
Chlorophyll a/b ratio
1.6
1.4
1.2
1
0.8
0.6
0.4
0.2
0
N.D.
SGR/WT Mock
SGR/nyc1 nol Mock
SGR/WT DEX
SGR/nyc1 nol DEX

Fig. 5

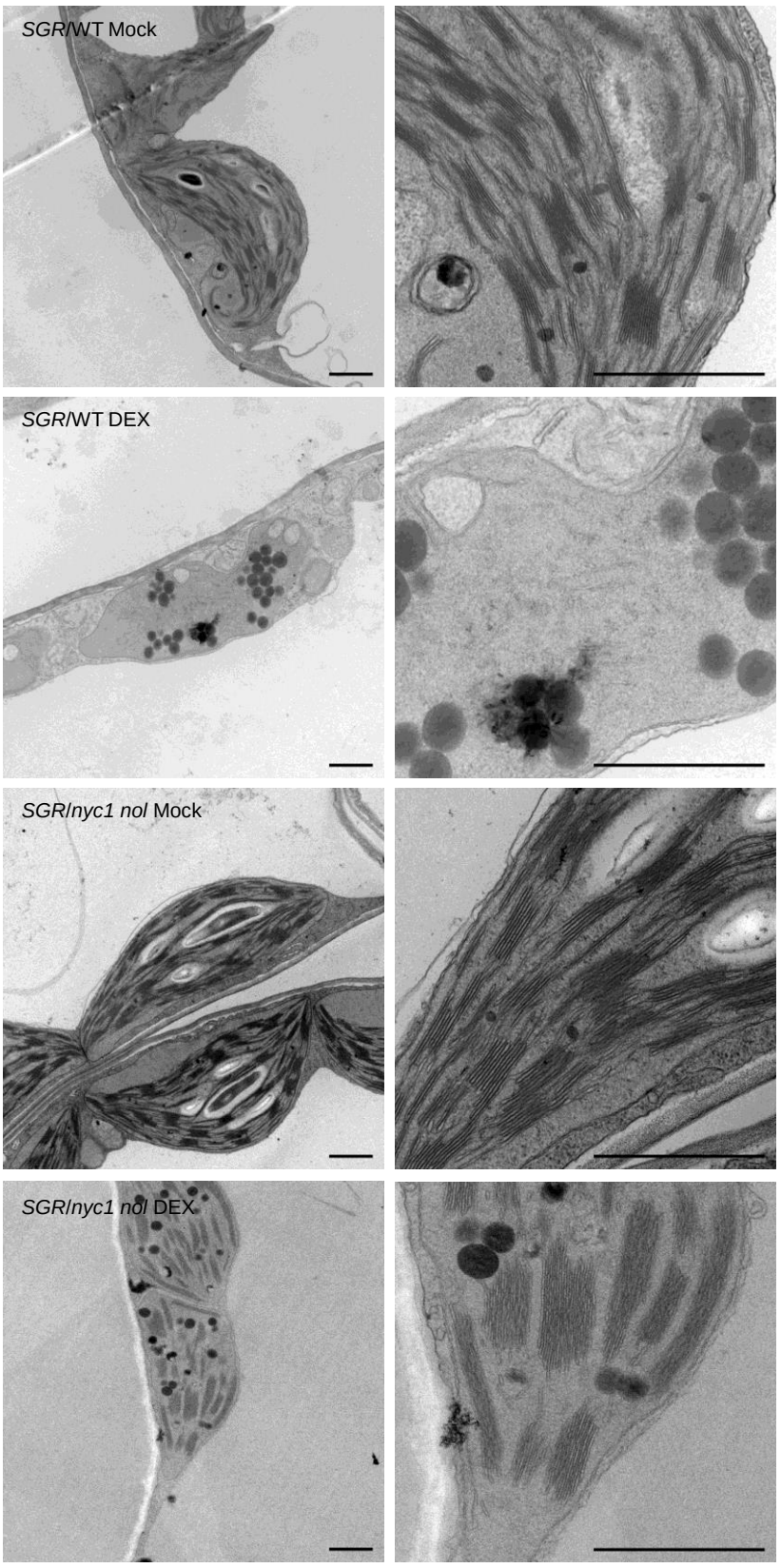

Fig. 6

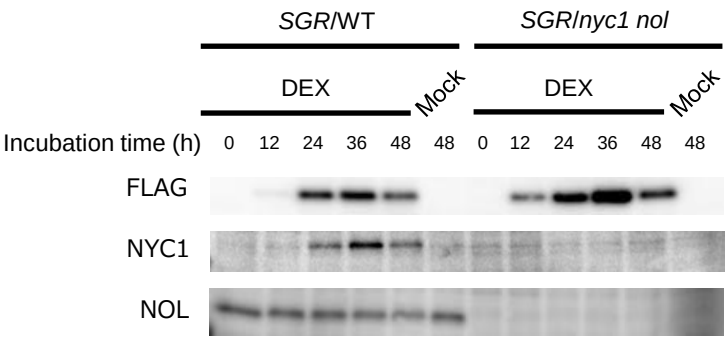
SGR/WT
SGR/nyc1 nol
DEX
Mock
DEX
Mock
Incubation time (h)
0 12 24 36 48 48 0 12 24 36 48 48
FLAG
NYC1
NOL

Fig. 7

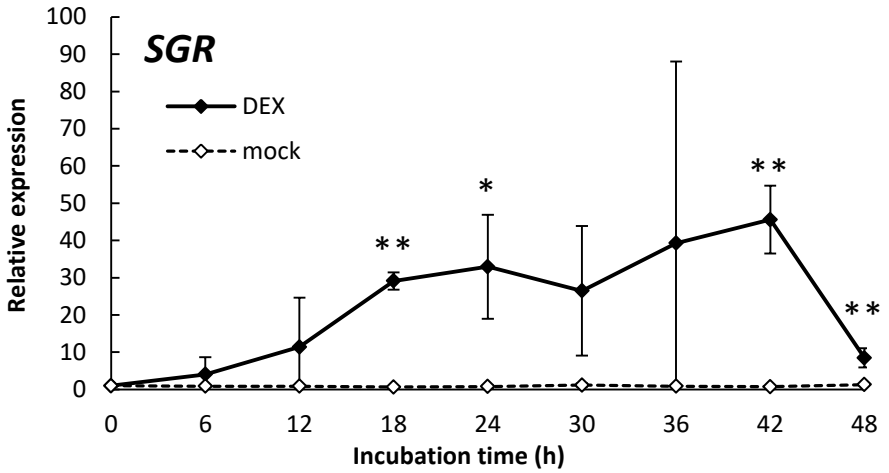
SGR
DEX
mock
Relative expression
Incubation time (h)
100
90
80
70
60
50
40
30
20
10
0
0
6
12
18
24
30
36
42
48
* *
*
* *
* *

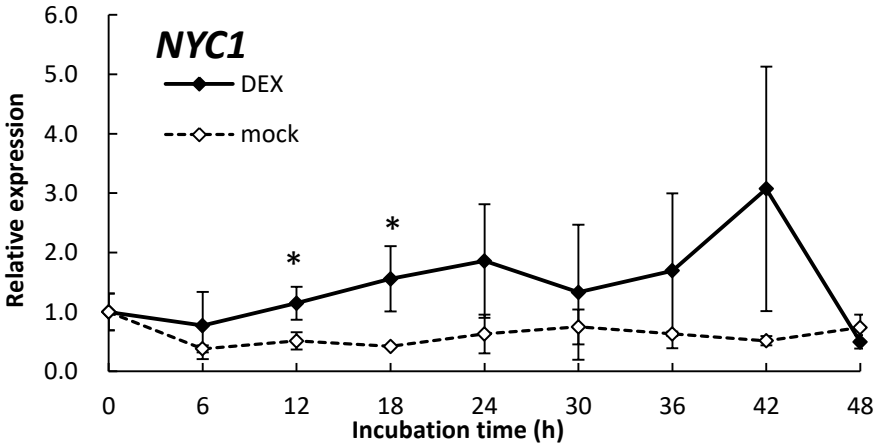
NYC1
DEX
mock
Relative expression
Incubation time (h)
6.0
5.0
4.0
3.0
2.0
1.0
0.0
0
6
12
18
24
30
36
42
48
*
*

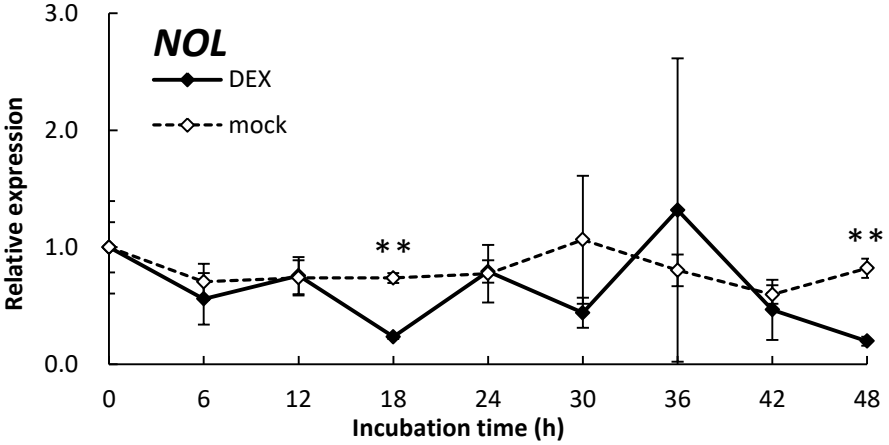
NOL
DEX
mock
Relative expression
Incubation time (h)
3.0
2.0
1.0
0.0
0
6
12
18
24
30
36
42
48
* *
* *

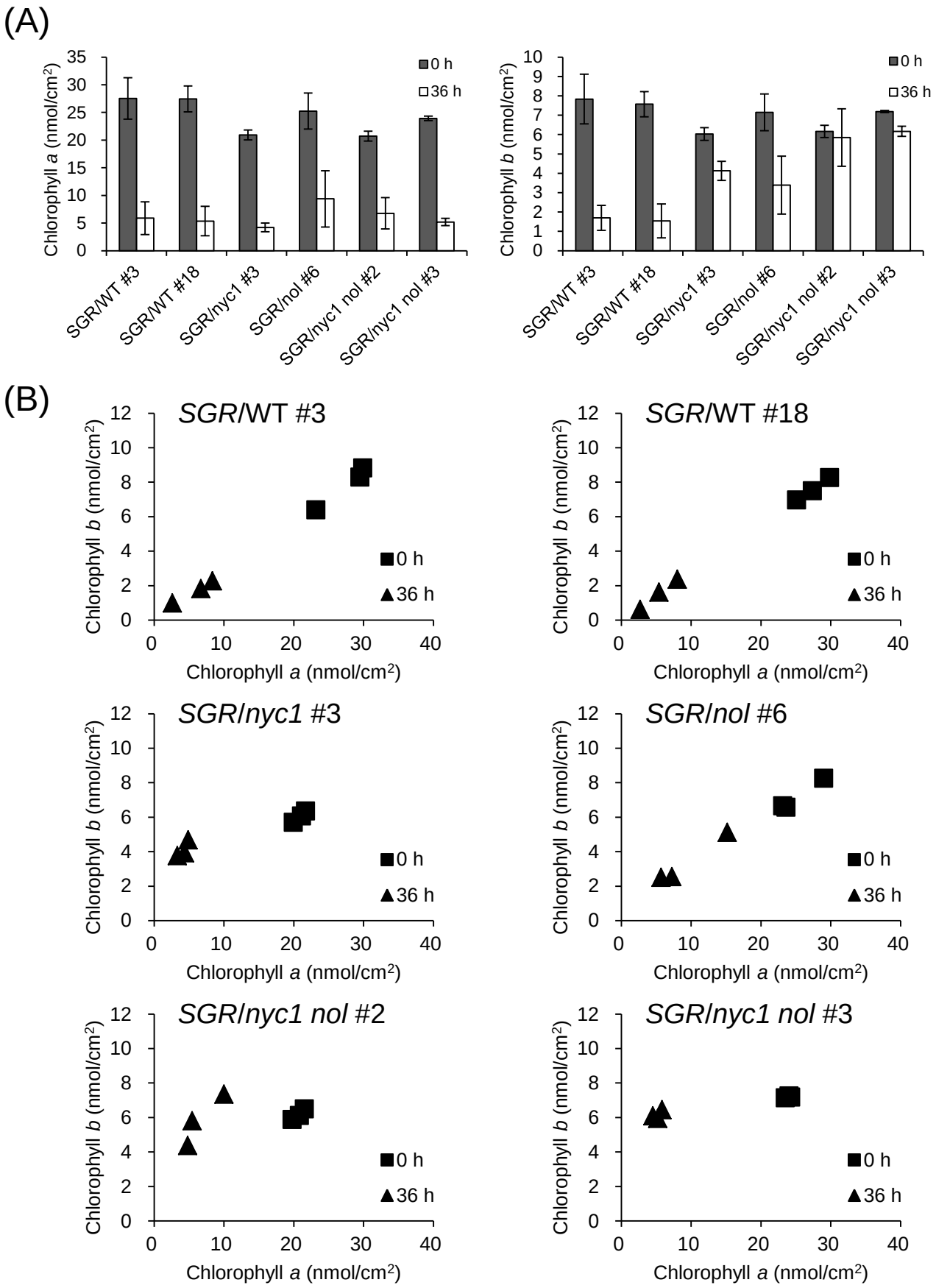

Supplemental Fig. S1 Chlorophyll content after DEX treatment
(A) Chlorophyll was extracted from leaf disks after 0 or 36 h of DEX treatment. All of these lines are genetically independent. Chlorophyll content was normalized by leaf area. The error bars represent the S. D. (n = 3). (B) The chlorophyll *b* level against the chlorophyll *a* level after 36 h of DEX treatment.

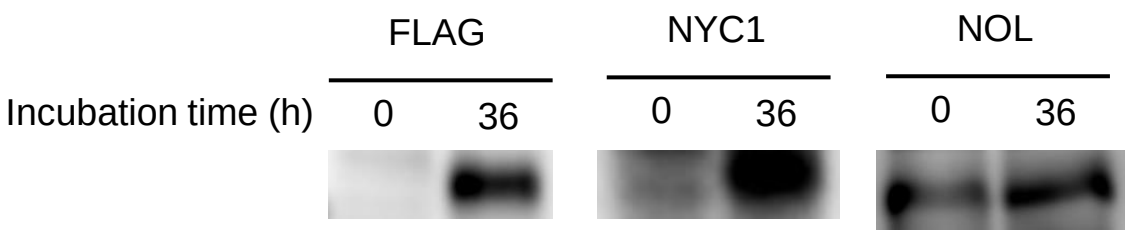

Supplemental Fig. S2 Protein accumulation after DEX treatment
Proteins were extracted from leaf disks of *SGR*/WT #3 after 0 or 36 h of DEX treatment. Results were normalized by leaf area. FLAG-tagged SGR was detected using a primary antibody against FLAG tag.